The Mediterranean Green Energy Forum 2013, MGEF-13

Maximum Efficiency or Power Tracking of Stand-Alone Small Scale Compressed Air Energy Storage System

Vorrapath Kokaew, Mohamed Moshrefi-Torbati, Suleiman M Sharkh*

Electro-Mechanical Research Group, Faculty of Engineering and the Environment, University of Southampton, UK

Abstract

This paper is concerned with maximum efficiency or power tracking for pneumatically-driven electric generator of a stand-alone small scale compressed air energy storage system (CAES). In this system, an air motor is used to drive a permanent magnet DC generator, whose output power is controlled by a buck converter supplying a resistive load. The output power of the buck converter is controlled power such that the air motor operates at a speed corresponding to either maximum power or maximum efficiency. The maximum point tracking controller uses a linearised model of the air motor together with integral control action. The analysis and design of the controller is based on a small injected-absorbed current signal-model of the buck converter. The controller was implemented experimentally using a dSPACE system. Test results are presented to validate the design and demonstrate its capabilities.

1. Introduction

Small scale compressed air energy storage systems (CAES), such as shown in Fig. 1, have the potential to provide an alternative energy storage system for renewable sources [1-4]. Although its energy density and efficiency are lower than lithium batteries, it has the advantage of being more environmentally friendly. Improved performance of the discharging process, using maximum efficiency point tracking (MEPT) algorithm, has recently been the focus of research [1, 2]. The maximum efficiency of an air motor usually occurs at a different speed from the maximum power point, and if maximum power is desired, then a different strategy maximum power point tracking (MEPT) strategy needs to be used.

---

* Corresponding author. Tel.: +44(0)23 8059 5568; fax: +44(0)23 8059 7051.
E-mail address: vk3e10@soton.ac.uk.

This paper discusses the design of both MEPT and MPPT for the CAES illustrated in Fig. 1. In this system, an air motor is used to drive a permanent magnet DC generator. The output power of the DC generator is controlled by a buck converter such that either MEPT or MPPT are achieved.
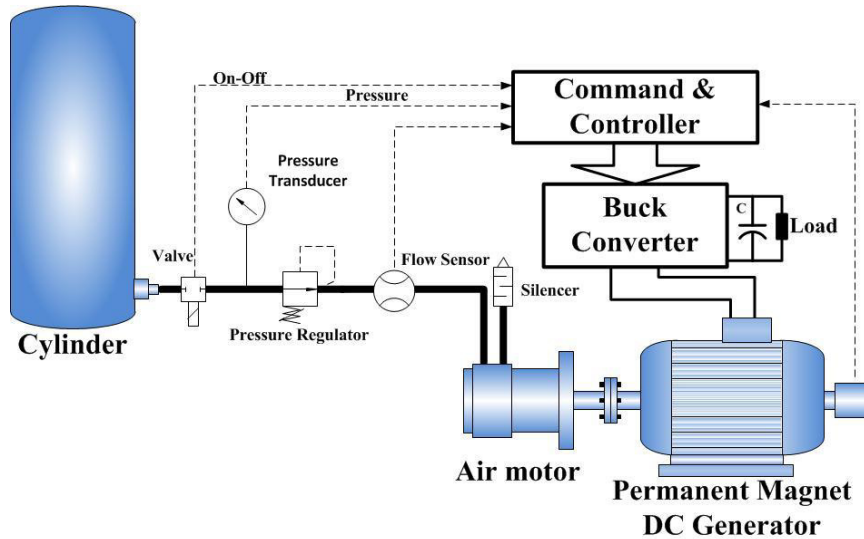

Fig. 1. Configuration of the proposed discharging process with MEPT/MPPT strategies

The paper starts by describing the modeling of a pneumatic to electrical energy conversion by modifying the existing curve fit equations of an air motor's air consumption [1] and by adapting a suitable model for a buck converter with a PM DC generator. The stability of the system is analysed based on a small signal model of the buck and a linearised model of the air motor. Finally, the paper discusses the practical implementation of the controller and presents experimental results.

2. System Model

In the following sections we derive linearised models of the air motor and buck converter and develop a model of the system.

2.1. Air motor model

In this work, the air motor LZB 14 AR034 (100W)[5] is utilized under variable inlet pressure (p_i). The motor can be characterised by toque (M_m), power (P_m) and air consumption ($\dot{V}_a$) using the following equations:

$$M_m = M_o\left(p_i\right)\left(1 - \frac{N_r}{N_o\left(p_i\right)}\right) \tag{1}$$

$$P_m = M_n(p_i)\frac{\pi}{30}\left(N_r - \frac{N_r^2}{N_o(p_i)}\right) \tag{2}$$

$$\dot{V}_a = \dot{V}_{max}(p_i)\exp\left(-\left(\frac{(N_r - c_1)}{c_2}\right)^2\right) \tag{3}$$

In these equations, the stall torque is $M_o(p_i) = c_{t1} \cdot p_i + c_{t2}$, the free speed is $N_o(p_i) = c_{n1}p_i^2 + c_{n2} \cdot p_i + c_{n3}$, and the maximum air consumption is $\dot{V}_{max}(p_i) = c_{a1} \cdot p_i + c_{a2}$, where, c_{t1}, c_{t2}, c_{n1}, c_{n2}, c_{n3}, c_{a1} and c_{a2} are real constants determined using curve fitting of the performance curves of the motor shown in Fig. 2. The maximum efficiency and maximum power lines clearly occur at different speeds as illustrated in Fig. 2. They are also strongly dependent on pressure.
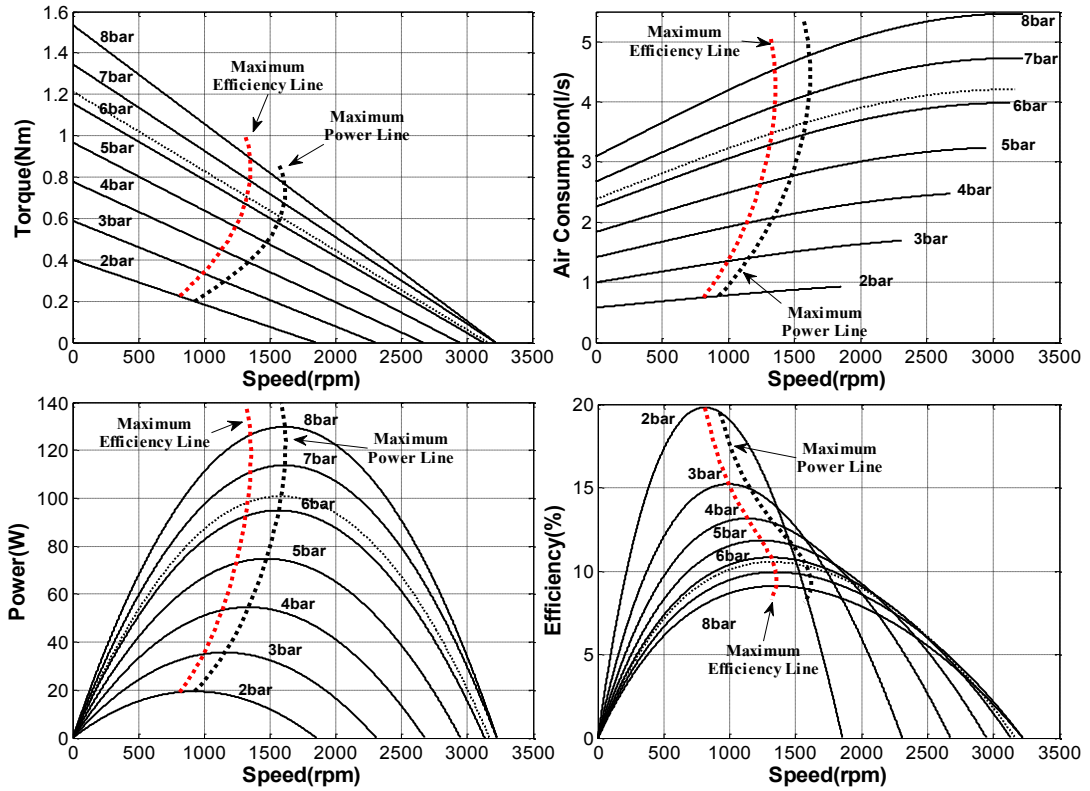

Fig. 2. Maximum efficiency and power lines on air motor characteristic curves

The derivative of shaft power of air motor (P_m) with respect to speed change is as below:

$$\frac{dP_m}{dN_r} = M_n(p_i)\frac{\pi}{30}(1 - 2\frac{N_r}{N_o(p_i)}) \tag{4}$$

Equating the above derivative to zero we obtain

$$N_r = \frac{N_o(p_i)}{2} \tag{5}$$

when the output power of the air motor is maximum.

The conversion efficiency of the air motor (η_{pm}) can be shown to be given by the ratio of the shaft power to the expanded air power at isentropic conditions[1],

$$\eta_{pm} = \frac{M_o\left(p_i\right)\dfrac{\pi}{30}\left(N_r - \dfrac{N_r^{\,2}}{N_o\left(p_i\right)}\right)}{\dfrac{\gamma}{\gamma-1}p_a\dot{V}_a\left[\left(\dfrac{p_i}{p_a}\right)^{\frac{\gamma-1}{\gamma}} - 1\right]} \tag{6}$$

The derivative of the conversion efficiency in (6) can be expressed as,

$$e \quad = \quad \frac{d\eta_{pm}}{dN_r} \quad = \quad K_1\left(1 - K_2 N_r\right) \tag{7}$$

where the K_1 and K_2 are defined as:

$$K_1 \quad = \quad \frac{M_o(p_i)\dfrac{\pi}{30}}{\dfrac{\gamma}{\gamma-1}p_a\dot{V}_a\left[\left(\dfrac{p_i}{p_a}\right)^{\frac{\gamma-1}{\gamma}} - 1\right]} \qquad \text{and} \qquad K_2 \quad = \quad \frac{2}{N_o(p_i)}$$

In the frequency domain (7) will be transformed to:

$$sE(s) \quad = \quad K_1 U(s) - K_1 K_2 N_r(s) \tag{8}$$

2.2. Model of permanent magnet DC generator and buck converter

PM DC generator – buck converter equivalent circuit is shown in Fig. 3. The Figure also shows the equivalent circuits when the buck switch is either on or off.

The dynamic behavior of the PM DC generator driven by a prime mover (air motor) is obtained by Newton's 2nd law, as

$$T_{am} - \left(B_{mam} + B_{mg}\right)\omega_{ram} - T_{eg} = \left(J_{am} + J_g\right)\frac{d\omega_{ram}}{dt} \tag{9}$$

The back emf (torque) constant of the generator is given by

$$E_{ag} \quad = \quad K_m \omega_{ram} \tag{10}$$

The load torque for the air motor is the generator's electromagnetic torque, i.e.,

$$T_{eg} = K_e\, i_{ag} \tag{11}$$

where i_{ag} is the generator armature current; ω_{ram} is the angular velocity of the air motor and the generator; r_{ag} is the armature resistance; L_{ag} is the inductance of the generator rotor winding, V_t is terminal voltage; K_e is torque constant; K_m is speed constant; B_{mam} and B_{mg} are the viscous friction coefficients of the air motor and the generator respectively and J_{am} and J_g are the moments of inertia of the air motor and the generator.
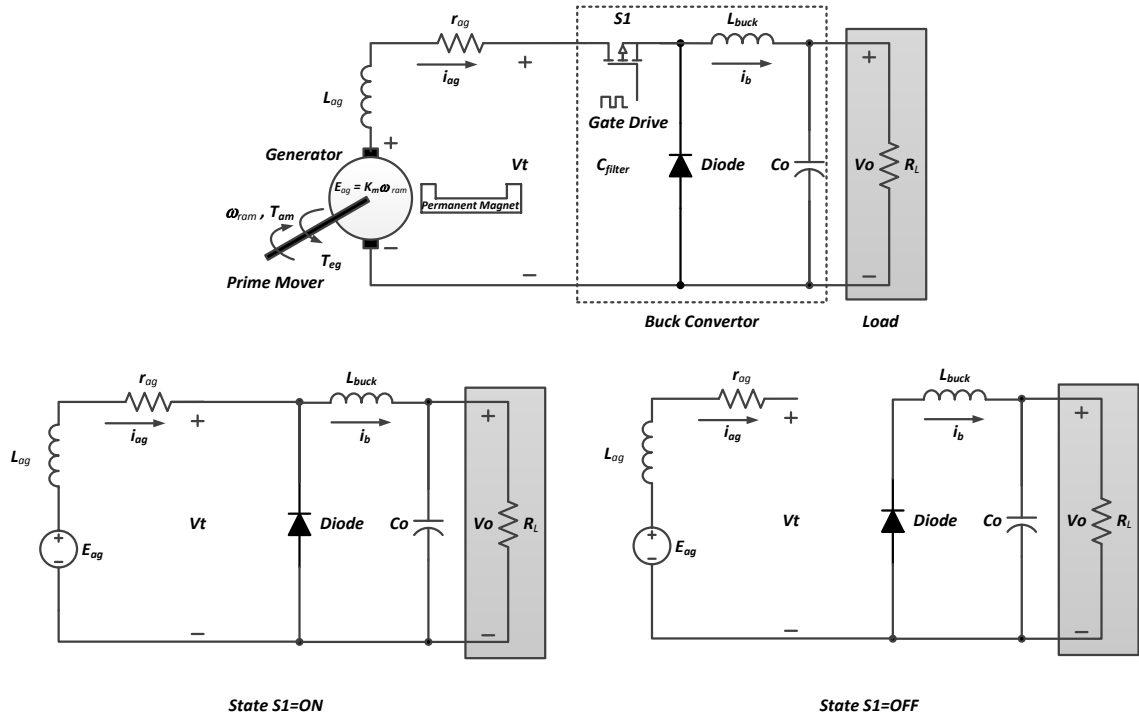
Fig. 3. Circuit schematic of PM DC generator-buck converter and equivalent circuit state ON-OFF

The average output voltage V_o of a buck converter is lower than its input voltage V_t depending on the duty cycle D of the switch S_1,

$$D = \frac{V_o}{V_t} \tag{12}$$

The Injected-absorbed current method [6] is applied to produce a small signal model of the buck converter as shown in Fig. 4. In this Figure $G_1(s)$, $G_2(s)$ and $G_3(s)$ are given by

$G_1(s) = (D/ (2\tau\, L_t))\, (\tau\, T\, (2\text{-}D) + ((2\tau\text{-}2DT+TD^2)/ (s+ (D/\tau))),$

$G_2(s) = (-1/(2\tau))[(\ \tau\ T(\ ((2D-D^2)/L_t)+((1-D)^2/L_{buck}))+((D/L_t)+((1-D)/L_{buck}))((2\tau-2DT+TD^2)/\ (s+\ (D/\tau))))]$,

$G_3(s) = T\ [((2-D)/2)\ (((E_{ag}-V_o)/L_t)-(I_m/\tau))\ +\ (D\ I_m/2\tau)-D\ ((E_{ag}-V_o)/2L_t)\ +\ (V_o\ (1-D)/L_{buck})]$
$\qquad + (1/\ (2\tau))\ [((E_{ag}-V_o)/L_t)\ -\ (I_m/\tau)\ +\ (V_o/L_{buck})]\ [((2\tau-2DT+TD^2)/\ (s+\ (D/\tau)))]$,

τ is the time constant (L_t/r_{ag}), L_t is the sum of L_{buck} and L_{ag} , I_m is the minimum inductor current (>0) and T is time period of switching.

The rate of power generation to storage conversion is then estimated based on equation (12) and further simplified in term of the armature and inductor currents, as given below

$$I_{ag}(s) \ = \ DI_b(s) \tag{13}$$

The relationship between the inductor current and the combination of the storage capacitor C_o and R_L in parallel is

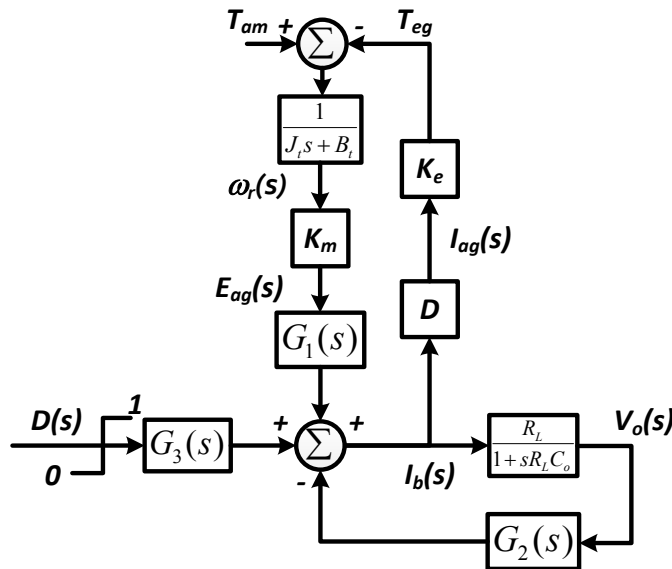$$I_b(s) \ = \ \left(\frac{R_L}{1+sR_LC_o}\right)V_o(s) \tag{14}$$

Fig. 4. Block diagram of the transfer function of PM-DC generator with buck converter

3. The Maximum Point Controller

The MEPT/MPPT controller is shown in Fig. 5. The user can select either MPPT or MEPT. When the MPPT is selected, the speed reference of the regulator is set to be half the free speed for the measured pressure according to equation (5). When the MEPT is selected, the reference speed is set such that the derivative of the efficiency is calculated using equations (7) and (8).
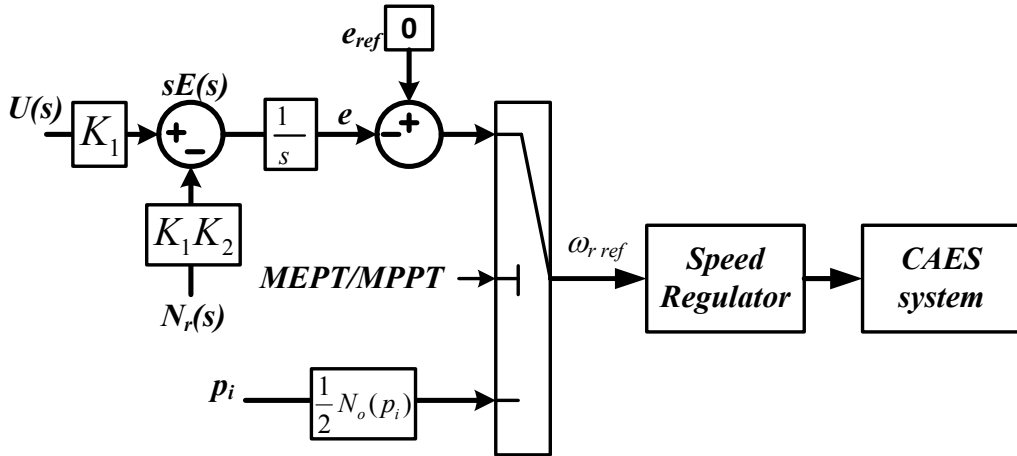
Fig. 5. The MEPT/MPPT controller

The reference speed is used to set the duty cycle of the buck converter as shown in Fig. 6. The speed regulator has 3 feedback loops of the actual speed, buck inductor current and the load voltage.
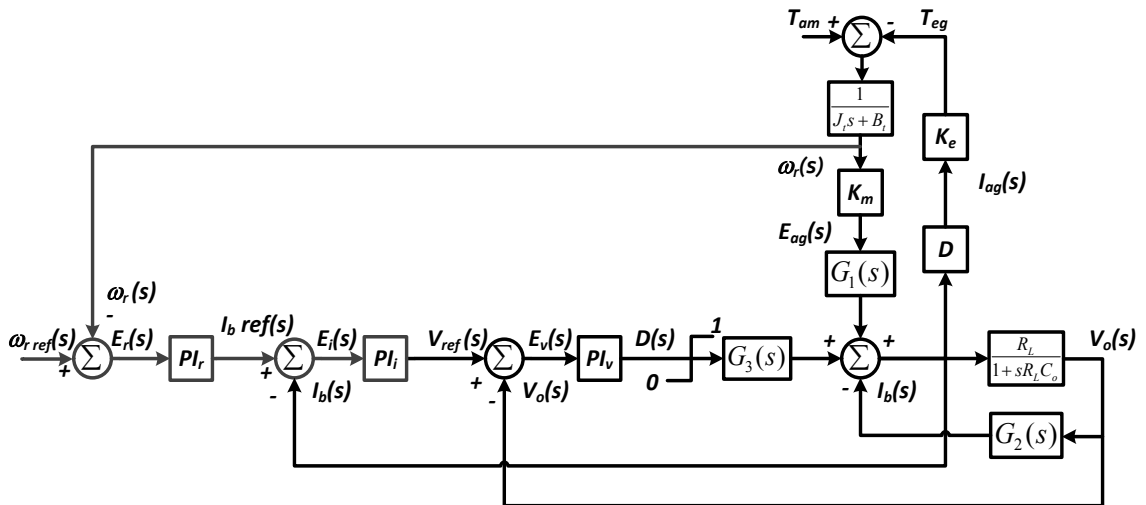

Fig. 6. The speed regulator controller

4. Experimental Implementation and Results

The proposed discharging process with MEPT/MPPT strategies in stand-alone was implemented using a dSPACE MicroAutobox II System that can be programmed graphically using Matlab-Simulink. The PM DC generator used was a LEMAC/65167-008, (24V, 3000 rpm, 250 W). An Atlas Copco LZB 14 AR034 (100W) was directly coupled to the generator. Data from the speed sensor, pressure transducer and flow sensor were sampled at a frequency of 20 kHz. A 100 VA the buck converter used a MOSFET

switching at 10 kHz. The load resistance R_L was nominally 0.25 Ω, but it can be switched to have that value during the test. The systems parameters are shown in Table 1.
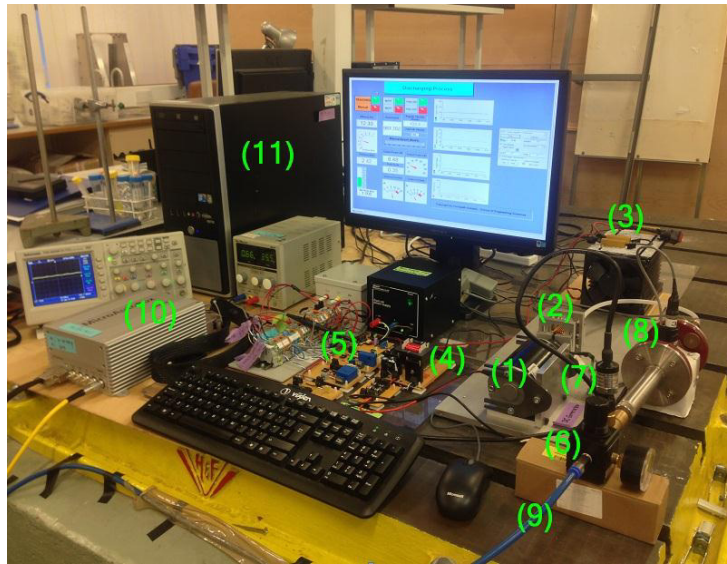
(1). Permanent Magnet DC Generator
(2). Air Motor
(3). Resistive Load
(4). Buck Converter
(5). Voltage and Current Sensors
(6). Pressure Regulator
(7). Pressure Transducer
(8). Flow Sensor
(9). Inlet Air Pressure
(10). dSPACE
(11). PC Computer

Fig. 7. Experimental rig in discharging process with MEPT/MPPT strategies in stand-alone system

The results in Fig. 8 show the response of the system under different load conditions for both MEPT and MPPT modes of operation. It is clear that the reference speed needed to achieve maximum efficiency is different from that needed to achieve maximum power. The results also show that the system is capable of coping with variable load conditions. Fig. 9 shows good agreement between the theoretical and experimental maximum power and maximum efficiency operating lines.

Table 1. System parameter values

| Description	Symbol	Value
Armature resistance	r_{ag}	0.484 Ω
Inductance of the generator	L_{ag}	585 μH
Torque and speed constant	K_e , K_m	0.086
Total moments of inertia	J_t	0.001125 kg.m^2
Viscous friction coefficients	B_t	0.001144 Nm s/rad
Inductance of the buck converter[7]	L_{buck}	157 μH
Capacitor of the buck converter[7]	C_o	11 μF
Atmospheric pressure	P_a	10^5 Pa
Ratio of specific heat	γ	1.4
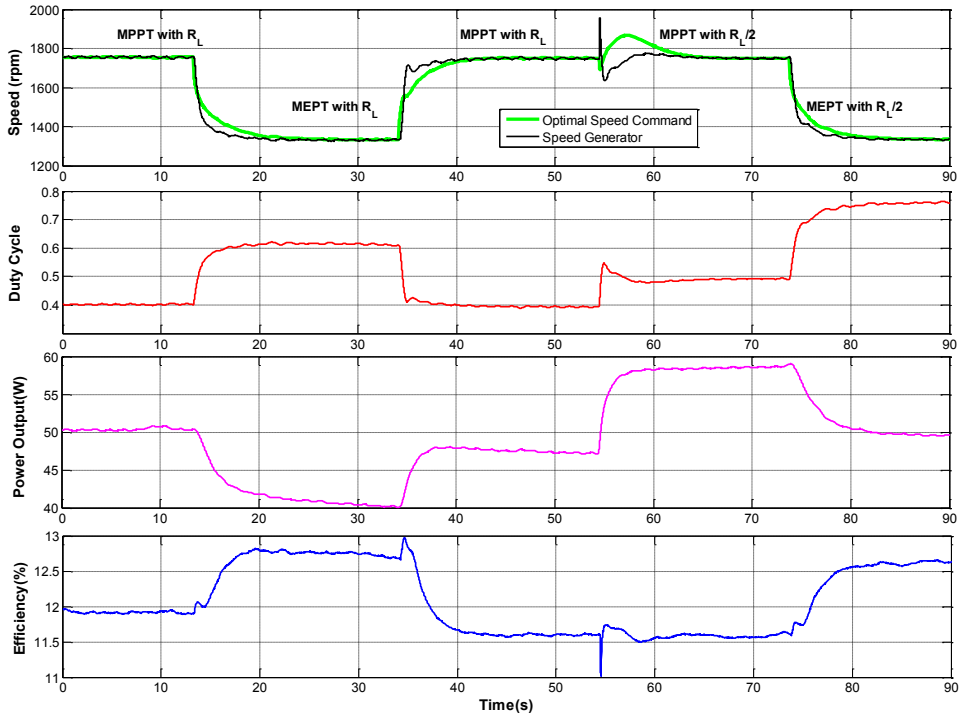
Fig. 8. Response of the system under MPPT and MEPT strategies with different load at constant inlet pressure of 6 bar
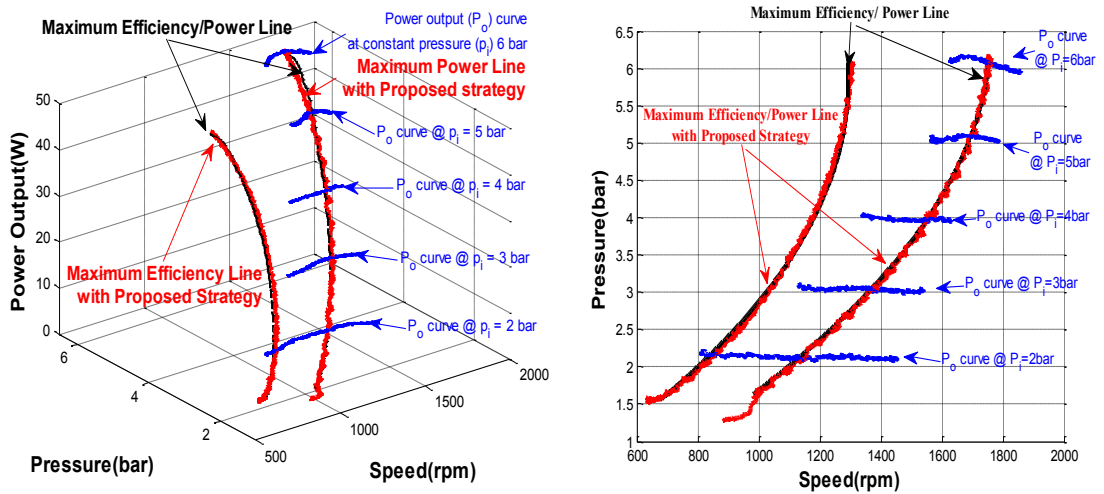
Fig. 9. Experimental and theoretical maximum power and maximum efficiency operating lines

5. Conclusion

To track maximum power, the reference speed of the air motor needs to be half of the free speed for a given pressure. The air motor speed corresponding to maximum efficiency can be also calculated from the motor characteristics and measurement of speed and pressure. These strategies were validated experimentally. However, these strategies require careful characterization of the air motor and require the use of speed and pressure sensors. Future work will investigate alternative strategies that do not require air motor characterization and use fewer sensors.

Acknowledgements

References

[1] Lemofouet-Gatsi S. Investigation and optimisation of hybrid electricity storage systems based on compressed air and supercapacitors: EPFL, 2006.

[2] Lemofouet S, Rufer A. A Hybrid Energy Storage System Based on Compressed Air and Supercapacitors With Maximum Efficiency Point Tracking (MEPT). Industrial Electronics, IEEE Transactions on. 2006;53(4):1105-15.

[3] Kokaew V, Moshrefi-Torbati M, Sharkh SM. Simulation of a solar powered air compressor. Environment and Electrical Engineering (EEEIC), 2011 10th International Conference on. 2011:1-4.

[4] Barrade P, Delalay S, Rufer A. Direct Connection of Supercapacitors to Photovoltaic Panels With On-Off Maximum Power Point Tracking. Sustainable Energy, IEEE Transactions on. 2012;3(2):283-94.

[5] Copco A. Air Motors.[Online].Available: http://www.atlascopco.com/airmotors/productrange/selectiontool/ [Accessed October,1 2011].

[6] Kislovski AS, Redl R, Sokal NO. Dynamic analysis of switching-mode DC/DC converters. New York: Van Nostrand Reinhold, 1991.

[7] Ang S, Oliva A. Power-Switching Converters, Second Edition: Taylor & Francis, 2005.